Interplay between phonon and impurity scattering in two-dimensional hole transport

Hongki Min,[1,2] E. H. Hwang,[2] and S. Das Sarma[2]

[1]*Department of Physics and Astronomy, Seoul National University, Seoul 151-747, Korea*

[2]*Condensed Matter Theory Center, Department of Physics, University of Maryland, College Park, Maryland 20742, USA*

(Received 13 March 2012; revised manuscript received 7 June 2012; published 9 August 2012)

We investigate temperature-dependent transport properties of two-dimensional p-GaAs systems taking into account both hole-phonon and hole-impurity scattering effects. By analyzing the hole mobility data of p-GaAs in the temperature range 10 K $< T <$ 100 K, we estimate the value of the appropriate deformation potential for hole-phonon coupling. Due to the interplay between hole-phonon and hole-impurity scattering the calculated temperature-dependent resistivity shows interesting nonmonotonic behavior. In particular, we find that there is a temperature range (typically 2 K $< T <$ 10 K) in which the calculated resistivity becomes independent of temperature due to a subtle cancellation between the temperature-dependent resistive scattering contributions arising from impurities and phonons. This resistivity saturation regime appears at low carrier densities when the increasing resistivity due to phonon scattering compensates for the decreasing resistivity due to the nondegeneracy effect. This temperature-independent flat resistivity regime is experimentally accessible and may have already been observed in a recent experiment.

DOI: 10.1103/PhysRevB.86.085307 PACS number(s): 72.10.Di, 73.40.−c, 73.63.−b

I. BACKGROUND

The room-temperature resistivity of a metal (as well as most metallic electronic materials, e.g., doped semiconductors) is mainly limited by the electron-phonon interaction,[1] i.e., by phonon scattering, with a notable exception being doped graphene with its very weak electron-phonon coupling.[2] The electron-phonon scattering contribution to the resistivity falls off strongly at very low temperatures ($T < T_{BG}$) in the so-called Bloch-Grüneissen (BG) regime,[1] due to the exponential suppression of the bosonic thermal occupancy of the phonons. At low temperatures therefore the electronic conductivity of metallic systems is invariably limited by disorder, i.e., by electron-impurity scattering, which gives rise to the zero-temperature residual resistivity of metals at low temperatures where the phonon scattering contribution has vanished. In general, the impurity scattering contribution to the metallic resistivity is temperature independent, at least in three-dimensional (3D) metals, because the impurities are quenched, and the temperature scale is therefore the Fermi temperature ($T_F \sim 10^4$ K in 3D metals), the impurity scattering contribution to the resistivity is essentially temperature independent in the 0–300-K regime. This, however, is not true if T_F is low as it could be in 2D semiconductor-based systems with their tunable carrier density where at low densities T_F could be just a few K. In fact, for 2D GaAs hole systems (2DHS), the situation with $T_F < 1$ K can easily be reached for a 2D hole density $\sim 10^{10}$ cm^{-2}.[3,4] This situation, which has no known analog in 3D metallic systems, leads to very strong experimentally observed temperature-dependent 2DHS resistivity in the $T \lesssim$ 1-K temperature range arising entirely from electron-impurity scattering since the phonon scattering is completely thermally quenched at such low temperatures. As an aside, we note that the temperature dependence of 2D electronic resistivity arising from impurity scattering in 2D GaAs based electron systems is rather weak due to the much lower effective mass of 2D electrons ($m_e \sim 0.07 m_0$, where m_0 is the vacuum electron mass), leading to much higher T_F, compared with 2D holes ($m_h \sim 0.4 m_0$) in GaAs-based 2D heterostructures.

The goal of the current work is to explore the interplay between impurity scattering and phonon scattering in the temperature-dependent resistivity of 2DHS in GaAs-based 2D systems. At higher temperature ($\gtrsim$100 K), the GaAs carrier resistivity is completely dominated by longitudinal optical (LO) phonon scattering, which has been extensively studied[5] and is not a subject matter of interest here since the resistivity limited by LO-phonon scattering manifests the strong exponential temperature dependence $\sim e^{-\hbar\omega_{LO}/k_B T}$ with $\hbar\omega_{LO} \sim 36$ meV.

Our interest is in the interplay between acoustic-phonon scattering and impurity scattering in the low to intermediate temperature regime ($T \sim T_{BG} - T_F$) where both impurity scattering and acoustic-phonon scattering contributions to resistivity would show nontrivial temperature dependence. In particular, we are interested in the question of whether an interplay between the two scattering processes could lead to an approximately constant (i.e., temperature independent) resistivity over some intermediate temperature range (1 K $< T <$ 40 K). Part of our motivation comes from a recent experiment[6] which discovered such an intermediate-temperature "resistivity saturation" phenomenon in a 2D GaAs-based electron system in the presence of a parallel magnetic field (which presumably serves to enhance the electron effective mass due to the magneto-orbital coupling, thus reducing the Fermi temperature of the electron system[7]). A second motivation of our work is estimating the deformation potential coupling strength for hole-acoustic-phonon scattering in 2DHS in GaAs. It turns out that the electron-phonon deformation coupling is not known in GaAs, and a quantitative comparison between our theoretical results and experimental transport data could lead to an accurate estimation of the deformation potential coupling in the GaAs-based 2DHS. We mention in this context that the accurate evaluation of the electron deformation potential coupling in 2D GaAs systems is also based on a quantitative comparison of the experimental and theoretical transport data.[5,8]

The basic physics we are interested in (see Fig. 1) is a situation where the acoustic-phonon contribution to the

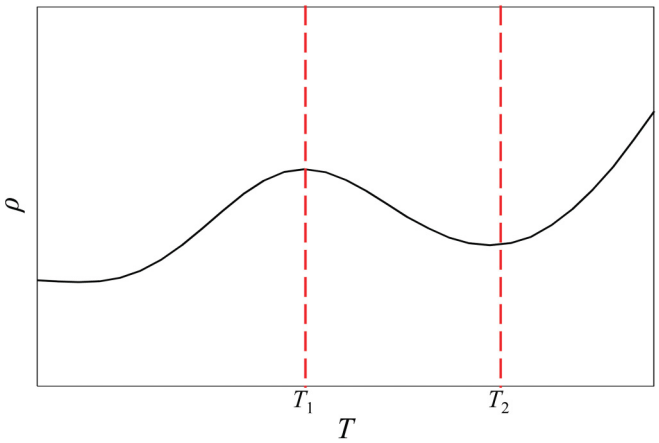

FIG. 1. (Color online) (a) Schematic resistivity behavior in the presence of both hole-impurity scattering and acoustic-phonon scattering as a function of temperature. Typically $T_1 \sim T_F$ and $T_2 \sim 5$–10 K depending on the carrier density.

resistivity increases linearly with increasing temperature ($T > T_{BG}$), but the impurity contribution decreases with increasing temperature ($T \gtrsim T_F$) as happens in a nondegenerate classical system where increasing temperature must necessarily increase the conductivity since the electrons are classically moving "faster." (We emphasize that such a situation is physically impossible in 3D metals since $T > 10^4$ K would be required, but is routinely achieved in 2D semiconductor-based systems where very low carrier density could lead to very low values of T_F.) We explicitly consider a situation with $T \ll T_{LO}$, where $T_{LO} \sim 100$ K in GaAs where LO phonons start contributing to the resistivity in a substantial manner. Now we ask the question of whether it is possible for the increasing temperature-dependent contribution to the hole resistivity arising from enhanced phonon scattering at higher temperatures could be approximately canceled over a finite temperature range by the decreasing temperature-dependent contribution arising from impurity scattering with increasing temperature due to the quantum-classical crossover, i.e., the nondegeneracy, effects. Some early theoretical work[9] indicated that the interplay between phonon scattering and nondegeneracy may indeed lead to a partial cancellation of different temperature-dependent contributions, producing an interesting nonmonotonicity (see Fig. 1) in the resistivity as a function of temperature in the 1–10-K range for low-density, high-mobility 2DHS in GaAs. In the current work, we look into this issue at great depth in view of the recent experimental work. In addition, we obtain the appropriate 2DHS deformation potential coupling constant by comparing our theoretical results to existing 2DHS hole transport data.

II. INTRODUCTION

The temperature-dependent transport in 2D systems has been a subject of intense activity since the observation of an apparent electronic metal-insulator transition (MIT), which represents the experimental observation of a transition from an apparent metallic behavior (i.e., $d\rho/dT > 0$, where ρ is the 2D resistivity) to an insulating behavior (i.e., $d\rho/dT < 0$) as the carrier density is reduced. The remarkable observation of the anomalous metallic temperature dependence of the resistivity is observed mostly in high-mobility low-density 2D semiconductor systems.[10,11] The low-temperature anomalous metallic behavior discovered in 2D semiconductor systems arises from the physical mechanism of strong temperature-dependent screening of charged impurity scattering.[10] At low temperatures ($T \lesssim T_F$, where $T_F = E_F/k_B$ is the Fermi temperature with the Fermi energy E_F) the main scattering mechanism in resistivity is due to impurity disorder from unintentional background charged impurities and/or intentional dopants in the modulation doping. The resistivity $\rho_{imp}(T)$ limited by the charged impurities increases linearly with temperature at lower temperatures ($T < T_F$) due to screening effects. This is a direct manifestation of the weakening of the screened charged disorder with increasing temperature[10,12] or equivalently an electron-electron interaction effect in the so-called ballistic regime.[13] For $T \gg T_F$, $\rho(T)$ decreases as T_F/T due to nondegeneracy effects and the quantum-classical crossover occurs at the intermediate temperature regime around $T \sim T_F$.[12]

The temperature-dependent resistivity[5] limited by acoustic phonons $\rho_{ph}(T)$ undergoes a smooth transition from a linear-T dependence at high ($T > T_{BG}$) temperatures to a weak high power T^a dependence with $a \geqslant 3$ as the temperature is reduced below $k_B T_{BG} = 2k_F v_{ph}$, where k_F is the Fermi wave vector of the 2D hole system and v_{ph} is the longitudinal or transversal sound velocity. The characteristic temperature T_{BG} is referred to as the Bloch-Grüneisen (BG) temperature. Note that T_{BG} is much smaller than the Debye temperature since the inverse lattice constant greatly exceeds k_F. In the BG regime ($T < T_{BG}$) the scattering rate is strongly reduced by the thermal occupation factors because the phonon population decreases exponentially and the phonon emission is prohibited by the sharp Fermi distribution, which gives rise to high power-law behavior ($a \geqslant 5$ with screening effects, but $a \geqslant 3$ without screening) in the temperature-dependent resistivity. Thus the phonon contribution to the resistivity is negligible compared to the charged impurities and the phonon contribution to the resistivity shows very weak temperature dependence for $T < T_{BG}$. For temperatures $T > T_{BG}$, since the electron-phonon scattering becomes proportional to the square of the oscillation amplitude of ions, the ρ_{ph} depends linearly on the temperature. We note that at low carrier density where k_F is small, T_{BG} can be very low.

In this paper we investigate the temperature-dependent transport properties of p-type GaAs-based 2DHSs for the temperatures $T \lesssim 100$ K by taking into account both hole-phonon and hole-impurity scatterings. In p-GaAs, holes interact with acoustic phonons through a short-range deformation potential as well as through a long-range electrostatic potential resulting from the piezoelectric effect. The precise value of the deformation-potential coupling constant D is very important to understand 2D p-GaAs carrier transport properties. For example, the mobility is strongly related to the deformation potential, $\mu \sim D^{-2}$. However, the precise value of D for p-GaAs has not been available, so the value of the n-GaAs deformation potential ($D = 12$ eV, Ref. 5) is used uncritically. Thus the current investigation of the transport properties of p-GaAs systems is motivated by getting the exact value of the deformation potential constant D in p-GaAs. We find that the

fitted value of deformation-potential coupling could change by as much as 60% (i.e., $D = 7.6$–12.7 eV) depending on the value of the depletion density $n_{\rm depl}$. When we assume $n_{\rm depl} = 0$, we obtain $D = 12.7$ eV as the most suitable value for the p-GaAs acoustic-phonon deformation coupling constant by fitting the available experimental data.[14] The value of $D = 12.7$ eV is larger than the generally accepted value in bulk GaAs ($D = 7$ eV),[15] but comparable to the value of the n-GaAs (12–14 eV).[8,16,17] However, due to the lack of knowledge about $n_{\rm depl}$ we have the uncertainty in the value of deformation potential coupling. To precisely determine the value of D for holes requires a careful measurement of $\rho(T)$ over the $T = 1$–50 K range in a high mobility and high density ($n \gtrsim 5 \times 10^{11}$ cm^{-2}) sample. Note that our finding of the apparent dependence of the GaAs 2D hole deformation potential coupling on the background (and generally unknown) depletion charge density in the 2DHS is obviously *not* a real effect since the hole-phonon coupling strength cannot depend on the depletion charge density. The apparent dependence we find arises from the fact that the calculated resistivity depends strongly on the depletion density whose precise value is unknown.

Other motivation of our work is to investigate the nontrivial nonmonotonic behavior of the temperature-dependent resistivity observed experimentally. In the presence of the hole-phonon and hole-impurity scattering a nonmonotonicity arises from a competition among three mechanisms:[4,9,18] screening which is particularly important for $T < T_{\rm F}$, nondegeneracy and the associated quantum-classical crossover for $T \sim T_{\rm F}$, and the phonon-scattering effect which becomes increasingly important for $T > 5$–10 K, depending on the carrier density. In Fig. 1 we show the schematic resistivity behavior of the p-GaAs in the presence of both charged impurity and phonon scatterings. At low temperatures ($T < T_1 \sim T_{\rm F}$), the scattering arising from charged impurities dominates and the resistivity increases as temperature increases due to the screening effects. For $T > T_2 \sim 5$–10 K the scattering by acoustic phonons plays a major role and limits the carrier mobility of p-GaAs systems in this temperature range. Note that in general $T_2 \gg T_{BG}$ for p-GaAs systems. However, at intermediate temperatures ($T_1 < T < T_2$) the competition between acoustic-phonon scattering and impurity scattering gives rise to a nontrivial transport behavior. We carefully study the nontrivial transport properties of p-GaAs in the intermediate temperature range (i.e., $T_1 < T < T_2$). Interestingly we find that the approximate temperature-dependent $\rho(T)$ in an intermediate temperature range can be constant, which arises from the approximate cancellation between the quantum-classical crossover and phonon scattering, and is quite general. When the phonon scattering dominates impurity scattering for $T > T_2$ the temperature dependence of hole mobility enables one to extract information on the electron-phonon scattering from mobility measurements. In this temperature range the valence-band deformation potential can be determined by fitting theoretical calculations to the existing carrier mobility data. In this paper we extract the value of the deformation potential by fitting the experimental mobility data, but uncertainty arises from the unknown values of the depletion charge density and background impurity charge density.

To investigate the temperature-dependent transport properties for the p-GaAs 2DHS we use the finite-temperature Boltzmann transport theory considering scatterings by charged random impurity centers and by electron-acoustic phonons with finite temperature and finite wave-vector screening through random-phase approximation (RPA).[10] We also include the finite-size confinement effects (i.e., we take into account the extent of the 2D system in the third dimension and do not assume it to be a zero-width 2D layer). The effect we neglect in our theory is the inelastic optical-phonon scattering. Polar carrier scattering by LO phonons is important in GaAs only at relatively high temperatures ($T \gtrsim 100$ K), becoming dominant at room temperatures. Due to the rather high energy of the GaAs optical phonons (∼36 meV), LO phonon scattering is completely suppressed in the temperature regime ($T < 100$ K) of interest to us in this work. Resistive scattering by optical phonons in the 2D GaAs system has been considered in the literature.[5] We note that the other scattering mechanisms (e.g., interface roughness scattering and alloy disorder scattering in $Ga_xAl_{1-x}As$, etc.) are known to be much less quantitatively important[19] than the mechanisms we are considering (i.e., impurity scattering and acoustic phonons) in this work.

The rest of the paper is organized as follows. In Sec. III we present the general theory of the impurity and phonon scatterings, and discuss the power-law behavior of the resistivity in the low- and high-temperature limit. In Sec. IV we show our calculated resistivity taking into account hole-phonon and hole-impurity scatterings, and demonstrate that there is a temperature-independent region due to the competition between the two scatterings. Finally we conclude in Sec. V summarizing our results.

III. THEORY

In this paper we use a single band (heavy-hole band) effective-mass approximation. In this model the complexities of all band details (including the spin-orbit interaction) are hidden in the effective mass. Our simple single-band model with the experimentally measured[20] effective mass ($m^* \sim 0.4m_0$, which is different from the theoretically proposed value[21]) has been widely used to avoid the complicated valence-band structures. In addition, it explains very well the transport experiments of 2D quantum well (heterostructure) systems at low hole densities.[9,14,22]

To investigate the temperature-dependent resistivity $\rho(T)$ [or equivalently conductivity $\sigma(T) \equiv \rho(T)^{-1}$] of p-GaAs systems we start with the Drude-Boltzmann semiclassical formula for 2D transport. Due to the finite extent in the z direction of the real 2D semiconductor system we have to include a form factor depending on the details of the 2D structure. In GaAs heterostructures, the carriers are spatially confined at the 2D interface and there is no longer translational invariance along the direction normal to the interface, designated as the z direction. We assume that the confinement profile is described by the variational wave function $\Psi(x,y,z) = \xi_0(z)e^{i(k_x x + k_y y)}$,[19] where

$$\xi_0(z) = \sqrt{\tfrac{1}{2}b^3z^2}\exp\left(-\tfrac{1}{2}bz\right), \qquad (1)$$

and b is a variational parameter. For a triangular well, b is given by[23]

$$b = \left(\frac{48\pi m^* e^2}{\epsilon_0 \hbar^2}\right)^{1/3} \left(n_{\rm depl} + \frac{11}{32} n\right)^{1/3}, \tag{2}$$

where m^* is an effective mass, ϵ_0 is the dielectric constant, $n_{\rm depl}$ is the depletion charge per unit area, and n is the 2D carrier density.

The density of states of 2DHS with parabolic energy dispersion $\varepsilon(\boldsymbol{k}) = \frac{\hbar^2 k^2}{2m^*}$ is given by

$$D(\varepsilon) = \begin{cases} D_0 & (\varepsilon > 0), \\ 0 & (\varepsilon < 0), \end{cases} \tag{3}$$

where $D_0 = \frac{g_s m^*}{2\pi\hbar^2}$ and $g_s = 2$ is the spin degeneracy factor. The carrier density n is given by

$$n = D_0 \int_0^\infty d\varepsilon f(\varepsilon) = D_0 k_{\rm B} T \ln\left[1 + \exp\left(\frac{\mu(T)}{k_{\rm B} T}\right)\right], \tag{4}$$

where $f(\varepsilon) = [e^{\beta(\varepsilon-\mu)} + 1]^{-1}$ is the Fermi distribution function and $\beta = 1/(k_{\rm B} T)$. Alternatively, the chemical potential $\mu(T)$ at a finite temperature T can be expressed as

$$\mu(T) = k_{\rm B} T \ln[\exp(E_{\rm F}/k_{\rm B} T) - 1], \tag{5}$$

where $E_{\rm F} = n/D_0$. Note that $\lim_{T\to 0} \mu(T) = E_{\rm F}$. From Eqs. (4) and (5),

$$\frac{\partial n}{\partial \mu} = D_0 \left[1 - \exp\left(-\frac{E_{\rm F}}{k_{\rm B} T}\right)\right]. \tag{6}$$

The finite temperature Thomas-Fermi (TF) screening wave vector $q_{\rm TF}(T)$ is defined by

$$q_{\rm TF}(T) = \frac{2\pi e^2}{\epsilon_0} \frac{\partial n}{\partial \mu} = q_{\rm TF} \left[1 - \exp\left(-\frac{E_{\rm F}}{k_{\rm B} T}\right)\right], \tag{7}$$

where $q_{\rm TF} = \frac{2\pi e^2}{\epsilon_0} D_0 = \frac{g_s e^2 m^*}{\epsilon_0 \hbar^2}$. Note that

$$q_{\rm TF}(T) = \begin{cases} q_{\rm TF} & (T \to 0), \\ q_{\rm TF}\left(\frac{E_{\rm F}}{k_{\rm B} T}\right) & (T \to \infty). \end{cases} \tag{8}$$

A. Electron-phonon interactions

The electron-longitudinal acoustic-phonon interaction Hamiltonian for a small phonon wave vector $\boldsymbol{Q}$ is

$$H_{\rm DP}(\boldsymbol{Q}) = D\, \boldsymbol{Q} \cdot \delta \boldsymbol{R}, \tag{9}$$

where D is the acoustic-phonon deformation potential and $\delta \boldsymbol{R}$ is the displacement vector. Note that the position operator in a simple harmonic oscillator with mass m and angular frequency ω is given by

$$x = \sqrt{\frac{\hbar}{2m\omega}}(a + a^\dagger), \tag{10}$$

where a and $a^\dagger$ are the annihilation and creation operators, respectively. Similarly, $\delta \boldsymbol{R}$ for $\boldsymbol{Q}$ can be expressed in terms of phonon annihilation and creation operators as

$$\delta \boldsymbol{R}(\boldsymbol{Q}) = \sqrt{\frac{\hbar}{2\rho_{\rm m}\omega_{\boldsymbol{Q}}}} \hat{e}_{\boldsymbol{Q}} (a_{\boldsymbol{Q}} + a^\dagger_{-\boldsymbol{Q}}), \tag{11}$$

where $\rho_{\rm m}$ is the mass density, $\omega_{\boldsymbol{Q}} = v_{\rm l} Q$, $v_{\rm l}$ is the longitudinal sound velocity, and $\hat{e}_{\boldsymbol{Q}}$ is the phonon polarization unit vector. Thus the electron-phonon interaction by the deformation potential coupling can be expressed as

$$H_{\rm ep} = D \sum_{\boldsymbol{Q}} \sqrt{\frac{\hbar}{2\rho_{\rm m}\omega_{\boldsymbol{Q}}}}\, \boldsymbol{Q} (a_{\boldsymbol{Q}} + a^\dagger_{-\boldsymbol{Q}}) \rho(\boldsymbol{Q}), \tag{12}$$

where $\rho(\boldsymbol{Q})$ is the electron density operator.

For the piezoelectric scattering in polar semiconductors (i.e., GaAs) the scattering matrix elements are equivalent to the substitution of the deformation with the following form:[24]

$$D^2 \to \frac{(e h_{14})^2 A}{Q^2}, \tag{13}$$

where h_{14} is the basic piezoelectric tensor component and A is a dimensionless anisotropy factor that depends on the direction of the phonon wave vector in the crystal lattice. We provide details of the parameter A in the following subsection.

B. Boltzmann transport theory

We calculate the temperature dependence of the hole resistivity by considering screened acoustic-phonon scattering. We include both deformation potential and piezoelectric coupling of the 2D holes to 3D acoustic phonons of GaAs. Details of the acoustic-phonon scattering theory are given in Ref. 5.

The transport relaxation time $\tau(\varepsilon_{\boldsymbol{k}})$ at an energy $\varepsilon_{\boldsymbol{k}}$ and a 2D wave vector $\boldsymbol{k}$ is given by

$$\frac{1}{\tau(\varepsilon_{\boldsymbol{k}})} = \int \frac{d^2 k'}{(2\pi)^2} W_{\boldsymbol{k},\boldsymbol{k}'} (1 - \cos\phi_{\boldsymbol{k}\boldsymbol{k}'}) \frac{1 - f(\varepsilon_{\boldsymbol{k}'})}{1 - f(\varepsilon_{\boldsymbol{k}})}, \tag{14}$$

where $W_{\boldsymbol{k},\boldsymbol{k}'}$ is the scattering probability between $\boldsymbol{k}$ and $\boldsymbol{k}'$ states, and $\phi_{\boldsymbol{k}\boldsymbol{k}'}$ is the scattering angle between $\boldsymbol{k}$ and $\boldsymbol{k}'$ vectors.

First, consider impurity scattering. Assume that impurity charges are distributed randomly in a 2D plane located at $(-d_{\rm imp})\hat{z}$ with a 2D impurity density $n_{\rm imp}$. Then the effective impurity potential for a 2D wave vector $\boldsymbol{q}$ is given by

$$\begin{aligned} V_{\rm imp}(\boldsymbol{q}, d) &= \int_0^\infty dz \xi_0^2(z) \left(\frac{2\pi e^2}{\epsilon_0 q} e^{-q(d_{\rm imp}+z)}\right) \\ &= \left(\frac{2\pi e^2}{\epsilon_0 q} e^{-q d_{\rm imp}}\right) \left(\frac{b}{b+q}\right)^3. \end{aligned} \tag{15}$$

From Fermi's "golden rule," $W_{\boldsymbol{k},\boldsymbol{k}'}$ for the impurity scattering has the following form:

$$W^{\rm imp}_{\boldsymbol{k},\boldsymbol{k}'} = \frac{2\pi}{\hbar} \frac{|V_{\rm imp}(\boldsymbol{q}, d)|^2}{\epsilon^2(\boldsymbol{q}, T)} n_{\rm imp} \delta(\varepsilon_{\boldsymbol{k}} - \varepsilon'_{\boldsymbol{k}}), \tag{16}$$

where $\boldsymbol{q} = \boldsymbol{k} - \boldsymbol{k}'$. The dielectric function $\epsilon(\boldsymbol{q}, T)$ takes into account the screening effects of electron gas at a wave vector $\boldsymbol{q}$ and a temperature T. We will consider screened scattering within RPA approximation defined by

$$\epsilon(\boldsymbol{q}, T) = 1 + \frac{q_{\rm s}(q, T)}{q}, \tag{17}$$

where $q_{\rm s}(q, T)$ is the temperature- and wave-vector-dependent screening wave vector.[25] In the long-wavelength limit ($q = 0$), $q_{\rm s}(q, T)$ is given by Eq. (7).

For electron-phonon scattering, $W_{\boldsymbol{k},\boldsymbol{k}'}$ for the electron-longitudinal acoustic-phonon interaction has the following form:[1]

$$W^{\rm ph}_{\boldsymbol{k},\boldsymbol{k}'} = \frac{2\pi}{\hbar}\int \frac{dq_z}{2\pi}\frac{|C(\boldsymbol{q},q_z)|^2}{\epsilon^2(\boldsymbol{q},T)}\Delta(\varepsilon_{\boldsymbol{k}},\varepsilon'_{\boldsymbol{k}})|I(q_z)|^2, \quad (18)$$

where $I_z(q_z)$ is the wave-function overlap at q_z defined by

$$I_z(q_z) = \int dz \xi_0^2(z) e^{iq_z z}. \quad (19)$$

Note that from Eq. (1), $|I_z(q_z)|^2 = \frac{b^6}{(b^2+q_z^2)^2}$.

The factor $C(\boldsymbol{q},q_z)$ is the matrix element for acoustic-phonon scattering. From Eq. (11), for the deformation potential (DP),

$$|C_{\rm DP}(\boldsymbol{q},q_z)|^2 = \frac{D^2\hbar Q}{2\rho_{\rm m} v_{\rm l}}, \quad (20)$$

while for the piezoelectric potential (PE),[5]

$$|C_{{\rm PE},\lambda}(\boldsymbol{q},q_z)|^2 = \frac{(eh_{14})^2\hbar A_\lambda(q,q_z)}{2\rho_{\rm m} v_\lambda Q}, \quad (21)$$

where $\boldsymbol{Q} = (\boldsymbol{q},q_z)$, $v_{\rm l}$ ($v_{\rm t}$) is the longitudinal (transverse) sound velocity and

$$A_{\rm l}(q,q_z) = \frac{9q_z^2q^4}{2\left(q_z^2+q^2\right)^3}, \quad A_{\rm t}(q,q_z) = \frac{8q_z^4q^2+q^6}{4\left(q_z^2+q^2\right)^3}. \quad (22)$$

The factor $\Delta(\varepsilon,\varepsilon')$ is given by

$$\Delta(\varepsilon,\varepsilon') = N_q\delta(\varepsilon-\varepsilon'+\hbar\omega_q) + (N_q+1)\delta(\varepsilon-\varepsilon'-\hbar\omega_q), \quad (23)$$

where $N_q = (e^{\beta\hbar\omega_q}-1)^{-1}$ is the phonon occupation number. Note that the first and second terms in Eq. (23) correspond to absorption and emission of phonons, respectively.

Finally, the total transport relaxation time is given by

$$\frac{1}{\tau_{\rm tot}(\varepsilon)} = \frac{1}{\tau_{\rm imp}(\varepsilon)} + \frac{1}{\tau_{\rm DP}(\varepsilon)} + \frac{1}{\tau_{{\rm PE,l}}(\varepsilon)} + \frac{2}{\tau_{{\rm PE,t}}(\varepsilon)}, \quad (24)$$

where in the last term the degeneracy of the transverse modes has been taken into account. Then electrical conductivity in a 2DHS is given by

$$\sigma = g_s e^2\int\frac{d^2k}{(2\pi)^2}\frac{v_{\boldsymbol{k}}^2}{2}\tau_{\rm tot}(\varepsilon_{\boldsymbol{k}})\left(-\frac{\partial f}{\partial\varepsilon}\right)_{\varepsilon=\varepsilon_{\boldsymbol{k}}}, \quad (25)$$

where $v_{\boldsymbol{k}}$ is the mean velocity at $\boldsymbol{k}$. By inverting the conductivity we have the resistivity, i.e., $\rho(T) = \sigma^{-1}(T)$.

C. Quasielastic limit

For a degenerate system ($k_{\rm B}T \ll E_{\rm F}$), all the scattering events at an energy ε take place in a thin shell around the energy circle and the scattering can be considered as quasielastic. For electron-phonon scatterings, the transport relaxation time in Eq. (14) is given by

$$\frac{1}{\tau(\varepsilon)} = \frac{2\pi}{\hbar}D_0\int\frac{d\phi}{2\pi}\int\frac{dq_z}{2\pi}\frac{|C(q)|^2}{\epsilon^2(q)}|I(q_z)|^2G(q)(1-\cos\phi), \quad (26)$$

where $q = 2k_{\rm F}\sin(\phi/2)$ and $G(q)$ is given by

$$\begin{aligned} G(q) &= \beta\int d\varepsilon f(\varepsilon)\{[1-f(\varepsilon+\hbar\omega_q)]N_q \\ &\quad + [1-f(\varepsilon-\hbar\omega_q)](N_q+1)\} \\ &= 2\beta\hbar\omega_q N_q(N_q+1). \end{aligned} \quad (27)$$

Thus for DP, Eq. (26) becomes[5,8]

$$\frac{1}{\tau_{\rm DP}(\varepsilon)} = \frac{3D^2m^*bk_{\rm B}T}{16\hbar^3\rho_{\rm m}v_l^2}\int_0^\pi\frac{d\phi}{\pi}\frac{(1-\cos\phi)}{\epsilon^2(q,T)} \times(\beta\hbar w_q)^2N_q(N_q+1), \quad (28)$$

while for PE,

$$\frac{1}{\tau_{{\rm PE},\lambda}(\varepsilon)} = \frac{c_\lambda(eh_{14})^2m^*k_{\rm B}T}{2\hbar^3\rho_{\rm m}v_\lambda^2}\int_0^\pi\frac{d\phi}{\pi}\frac{(1-\cos\phi)}{q\epsilon^2(q,T)} \times(\beta\hbar w_q)^2N_q(N_q+1)f_\lambda(q/b), \quad (29)$$

where $c_{\rm l} = 9/32$, $c_{\rm t} = 13/32$ and

$$\begin{aligned} f_{\rm l}(w) &= \frac{1+6w+13w^2+2w^3}{(1+w)^6}, \\ f_{\rm t}(w) &= \frac{13+78w+72w^2+82w^3+36w^4+6w^5}{13(1+w)^6}. \end{aligned} \quad (30)$$

For simplicity, consider the $f_\lambda(q/b) = 1$ case assuming $b \gg 1$ in the extreme 2D limit. Then, in the high-temperature limit,

$$\begin{aligned} \frac{1}{\tau_{\rm DP}(T)} &\approx \frac{3D^2m^*bk_{\rm B}T}{16\hbar^3\rho_{\rm m}v_l^2} \propto T, \\ \frac{1}{\tau_{{\rm PE},\lambda}(T)} &\approx \frac{c_\lambda(eh_{14})^2m^*}{2\hbar^3\rho_{\rm m}v_\lambda^2}\frac{4}{\pi}\frac{T}{T_{\rm BG}} \propto T, \end{aligned} \quad (31)$$

while in the low-temperature limit,

$$\begin{aligned} \frac{1}{\tau_{\rm DP}(T)} &\approx \frac{3D^2m^*bk_{\rm B}T}{16\hbar^3\rho_{\rm m}v_l^2}\frac{4\times6!\zeta(6)}{\pi x_{\rm TF}^2}\left(\frac{T}{T_{\rm BG}}\right)^5 \propto T^6, \\ \frac{1}{\tau_{{\rm PE},\lambda}(T)} &\approx \frac{c_\lambda(eh_{14})^2m^*}{2\hbar^3\rho_{\rm m}v_\lambda^2}\frac{4\times5!\zeta(5)}{\pi x_{\rm TF}^2}\left(\frac{T}{T_{\rm BG}}\right)^5 \propto T^5, \end{aligned} \quad (32)$$

where $x_{\rm TF} = q_{\rm TF}/(2k_{\rm F})$. Note that the resistivity is proportional to the inverse relaxation time, thus it follows the same power-law dependence in the high- or low-temperature limit.

For the charged impurity with temperature-dependent screening wave vector the asymptotic low- and high-temperature behaviors of 2D resistivity for a δ-layer system are given by[26]

$$\rho_{\rm imp}(T \ll T_{\rm F}) \sim \rho_0\left[1+\frac{2x_{\rm TF}}{1+x_{\rm TF}}\frac{T}{T_{\rm F}} + C\left(\frac{T}{T_{\rm F}}\right)^{3/2}\right], \quad (33)$$

$$\rho_{\rm imp}(T \gg T_{\rm F}) \sim \rho_1\frac{T_{\rm F}}{T}\left[1-\frac{3\sqrt{\pi}x_{\rm TF}}{4}\left(\frac{T_{\rm F}}{T}\right)^{3/2}\right], \quad (34)$$

where $\rho_0 = \rho(T=0)$, $\rho_1 = (h/e^2)(n_{\rm imp}/n\pi x_{\rm TF}^2)$, and $C = 2.646[x_{\rm TF}/(1+x_{\rm TF})]^2$. At low temperatures ($T < T_{\rm F}$) the resistivity increases linearly due to screening (or electron-electron interaction) effects on the impurity scattering.[10,12] To get the linear temperature-dependent resistivity at low temperatures it is crucial to include the temperature-dependent

screening wave vector.[10] At high temperatures ($T > T_F$) $\rho(T)$ decreases inverse linearly due to nondegeneracy effects. Thus it is expected that the resistivity has a maximum value and the quantumclassical crossover occurs at the intermediate-temperature regime around T_F. When we consider both hole-phonon and hole-impurity scatterings the temperature-dependent resistivity becomes nontrivial due to the competition between these two independent scattering mechanisms. Since the resistivity limited by charged impurities decreases at high temperatures, phonon scattering eventually takes over and $\rho(T)$ increases with T again, which gives rise to nonmonotonicity in $\rho(T)$. The nonmonotonicity becomes pronounced in the systems with strong impurity scattering or at low carrier density. For weaker impurity scattering the phonon scattering dominates before the quantum-classical crossover occurs, so the overall resistivity increases with temperature. At higher carrier densities, T_F is pushed up to the phonon-scattering regime, and the quantum-classical crossover physics is overshadowed by phonons so that nonmonotonicity effects are not manifest.

IV. NUMERICAL RESULTS

A. Determination of deformation potential

In this section we provide the numerically calculated temperature dependence of the hole resistivity by considering both screened acoustic-phonon scattering and screened charged impurity scattering. In the calculation of phonon scattering we use the parameters corresponding to GaAs: $m^* = 0.38\, m_e$, $v_l = 5.14 \times 10^5$ cm/s, $v_t = 3.04 \times 10^5$ cm/s, $\rho_m = 5.3$ g/cm^3, and $eh_{14} = 1.2 \times 10^7$ eV/cm. For the deformation potential, we fitted several available mobility data sets[14,27] and the best fitted value we obtained is $D = 12.7$ eV for $n_{depl} = 0$ (see Fig. 2). In the following calculations we use this value as a deformation potential of p-GaAs.

To obtain the best-fitted value of the deformation potential, in Fig. 2, we calculate the total mobility $\mu = \sigma/ne$ with Eqs. (24) and (25) as a function temperature for different values of the deformation-potential constant D. Knowing the

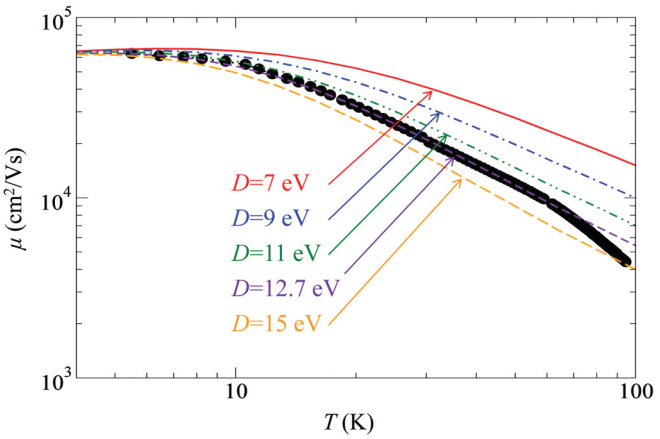

FIG. 2. (Color online) Mobility as a function of temperature for several values of D with $n = 2 \times 10^{11}$ cm^{-2}, $n_{imp} = 1.22 \times 10^{10}$ cm^{-2}, $n_{depl} = 0$ and $d_{imp} = 0$. Black dots represent the experimental data (Ref. 14).

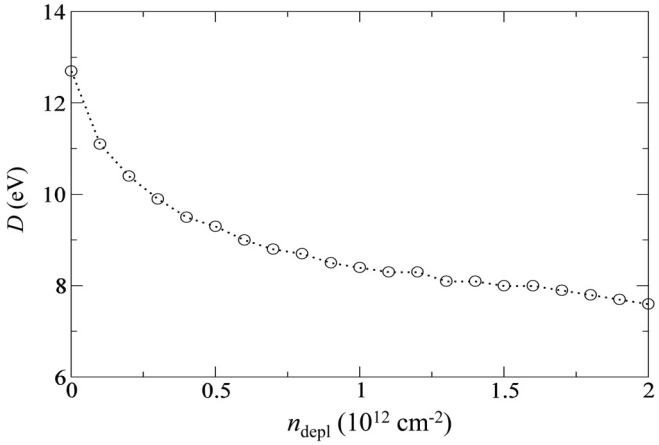

FIG. 3. Fitted deformation potential D as a function of depletion density n_{depl} for a sample with $n = 2 \times 10^{11}$ cm^{-2} and $d_{imp} = 0$.

precise value of the deformation-potential coupling constant D is very critical because $\mu \sim D^{-2}$, i.e., the calculated mobility will be uncertain by a factor of 4 with values of D differing by a factor of 2. In this calculation we consider two different scattering mechanisms: remote impurity scattering and acoustic-phonon scattering. We first fit the low-temperature data ($T \lesssim 4$ K) to find the charged impurity density, n_{imp}, because the phonon scattering is severely suppressed and the charged impurity scattering determines the carrier mobility in this temperature range. We set $d_{imp} = 0$ for simplicity and carried the effect of impurity by n_{imp}. For $n_{depl} = 0$, we find that $n_{imp} = 1.22 \times 10^{10}$ cm^{-2} gives the best fitted mobility at low temperatures for the data set. With this impurity density we calculate the mobility data at high temperatures (20 K $< T <$ 60 K) by changing deformation potential. From Fig. 2, we get $D = 12.7$ eV as the most suitable value for the p-GaAs acoustic-phonon deformation coupling constant.

In Fig. 3 we show the deformation potential coupling as a function of the depletion density for a hole density $n = 2 \times 10^{11}$ cm^{-2}. The calculated deformation potential D strongly depends on the depletion density n_{depl} for $n_{depl} < 10^{12}$ cm^{-2}, but for higher densities ($n_{depl} > 10^{12}$ cm^{-2} it decreases slowly, as seen in Fig. 3. n_{depl} is a measure of fixed charges in the background and typically n_{depl} is unknown. Thus the uncertainty in the value of deformation potential coupling (both for electrons and for holes) could be a result of our lack of knowledge about n_{depl}. When $n_{depl} = 0$ we get $D = 12.7$ eV. We use $D = 12.7$ eV in the remaining calculations with $n_{depl} = 0$. However, the different values of D do not change the results qualitatively.

B. Acoustic-phonon-limited transport

Using the theoretical model outlined in Sec. III we study hole transport limited by acoustic phonons in this subsection. In Fig. 4 we show the calculated scattering rates τ_s^{-1} and transport relaxation rates τ_t^{-1} due to acoustic phonons, as a function of the hole energy. The relevant transport relaxation rate, τ_t^{-1}, has been obtained in Eq. (26). The two characteristic times shown in Fig. 4 differ by the important $(1 - \cos\theta)$ factor.[28] The scattering rate τ_s^{-1} is given by making the replacement $(1 - \cos\theta) \to 1$ in the integrand for the formula

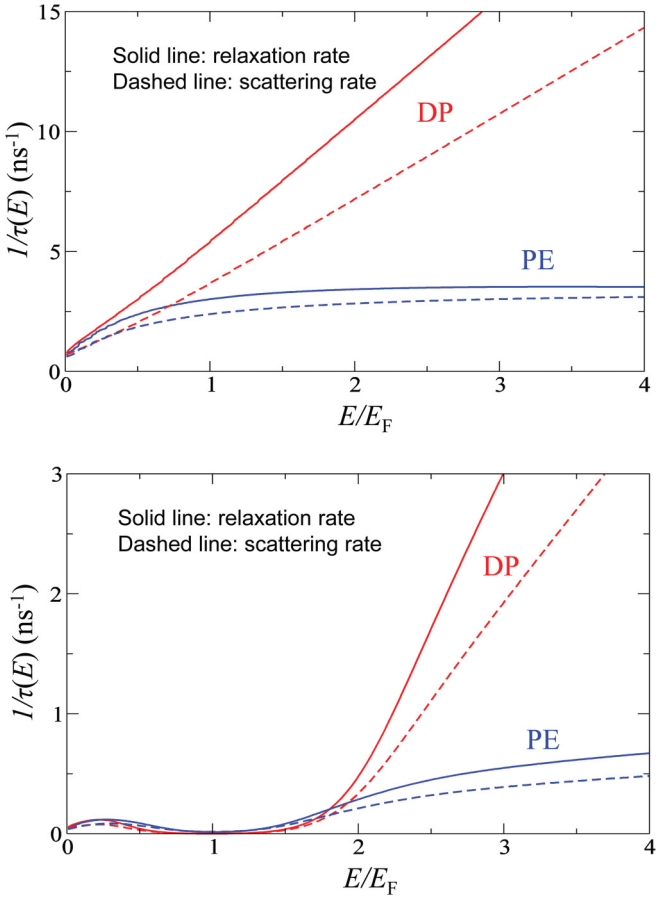

FIG. 4. (Color online) The relaxation rate (solid line) and scattering rate (dashed line) as a function of hole energy E for (a) $T = 10$ K and (b) $T = 1$ K with $n = 10^{11}$ cm^{-2}, $n_{\rm imp} = 0$, $n_{\rm depl} = 0$, and $D = 12.7$ eV. DP and PE represent the deformation potential and piezoelectric potential contributions, respectively.

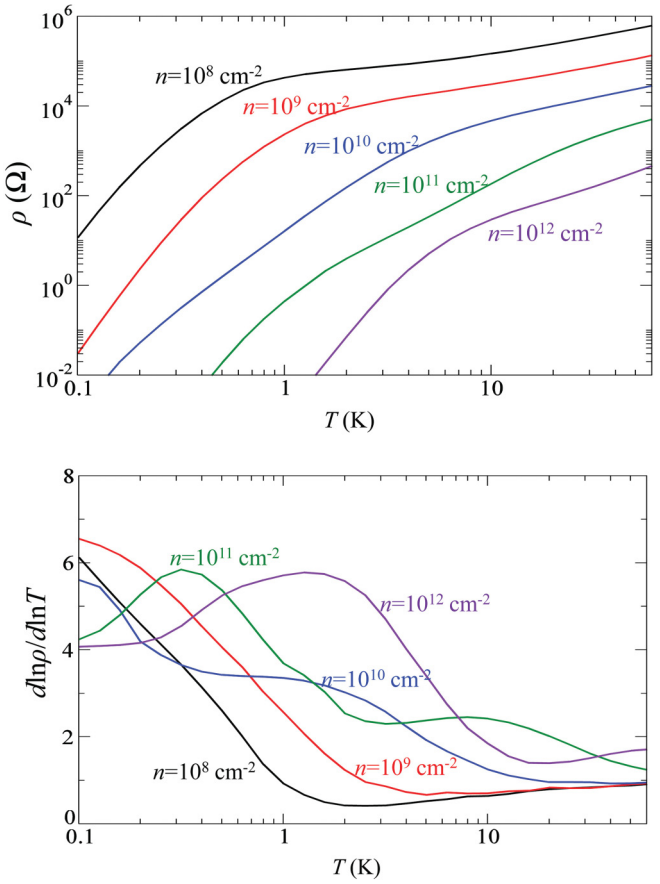

FIG. 5. (Color online) (a) Acoustic-phonon-limited resistivity of 2DHS as a function of temperature for $n = 10^8$, 10^9, 10^{10}, 10^{11}, 10^{12} cm^{-2} and (b) the calculated exponent a in $\rho(T) \propto T^a$ which is obtained from logarithmic derivatives of (a).

for τ_t^{-1} given in Eq. (26). τ_t determines the conductivity (or mobility), $\sigma = ne\mu = ne^2\tau_t/m$, where n is the carrier density and μ is the mobility, whereas τ_s determines the quantum level broadening, $\gamma = \hbar/2\tau_s$, of the momentum eigenstates. The scattering time τ_s is related to the imaginary part of the single-particle self-energy and simply gives the time between scattering events between a hole and an acoustic phonon. The difference between τ_t and τ_s arises from the subtle effect of the wave-vector-dependent transition rate.[28] The large-angle scattering events (or large momentum transfer) contribute significantly to the transport scattering events, but small-angle scattering events where $\cos\theta \approx 1$ makes a negligible contribution to τ_t, while all scattering events contribute equally to τ_s. Our result for the individual DP and total PE rates are given in Fig. 4 for $n = 10^{11}$ cm^{-2} at two different temperatures $T = 10$ K and $T = 1$ K. In this calculation we take $D = 12.7$ eV which is the best-fitted values of the experimental data. We find that $\tau_t/\tau_s \approx 1$, since the screened electron-acoustic mode phonon interactions are of relatively short range. It has been known that the ratio τ_t/τ_s from remote ionized impurities is much bigger due to the long-range nature of the electron-impurity interaction.[29]

Figure 5(a) shows acoustic-phonon-limited resistivity of 2DHS in the absence of impurity scattering as a function of temperature for different hole densities $n = 10^8$, 10^9, 10^{10}, 10^{11}, 10^{12} cm^{-2}. The calculated resistivities clearly demonstrate the two different regimes: BG region characterized by high power-law behavior for $T < T_{\rm BG}$ and equipartition region with $\rho \sim T$ behavior for $T > T_{\rm BG}$. The transition temperature $T_{\rm BG}$ increases with density since $T_{\rm BG} \propto \sqrt{n}$. As the density increases the calculated resistivity at a fixed temperature decreases. In Fig. 5(b) we show the logarithmic derivatives of the acoustic-phonon-limited resistivity, which give rise to an approximate temperature exponent of acoustic-phonon-limited resistivity by writing $\rho \sim T^a$, i.e., $a = d\ln\rho/d\ln T$. At the low-temperature BG regime $T < T_{\rm BG}$ the numerically evaluated exponent a varies from 4 to 6 depending on the carrier density. But at high temperatures the exponent approaches to 1 as we expected, i.e., $\rho(T) \propto T$.

Figure 6(a) shows acoustic-phonon-limited mobility of 2DHS in the absence of impurity as a function of temperature for different hole densities $n = 10^8, 10^9, 10^{10}, 10^{11}, 10^{12}$ cm^{-2}. At high temperatures ($T > 10$ K) the calculated mobilities show very weak density dependence for the density range $n = 10^{10}$–10^{12} cm^{-2} and decrease approximately as $\mu \sim T^{-1}$. Thus the reciprocal mobility increases linearly with temperature, i.e., $1/\mu = 1/\mu_0 + \alpha T$, where α is the slope in the relation between μ^{-1} and T. Figure 6(b) shows density dependence of the slope α for $n_{\rm imp} = 0$ and 5×10^9 cm^{-2} in

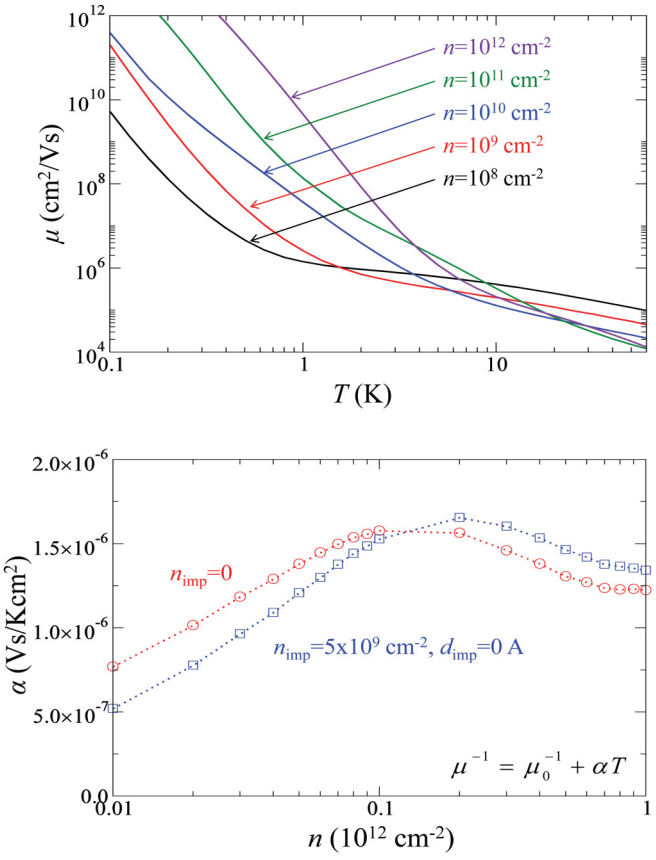

FIG. 6. (Color online) (a) Acoustic-phonon-limited mobility of 2DHS as a function of temperature for $n = 10^8$, 10^9, 10^{10}, 10^{11}, 10^{12} cm^{-2}. (b) Density dependence of coefficient α for $n_{imp} = 0$ and 5×10^9 cm^{-2}, where $1/\mu = 1/\mu_0 + \alpha T$ in 10 K $< T <$ 60 K range.

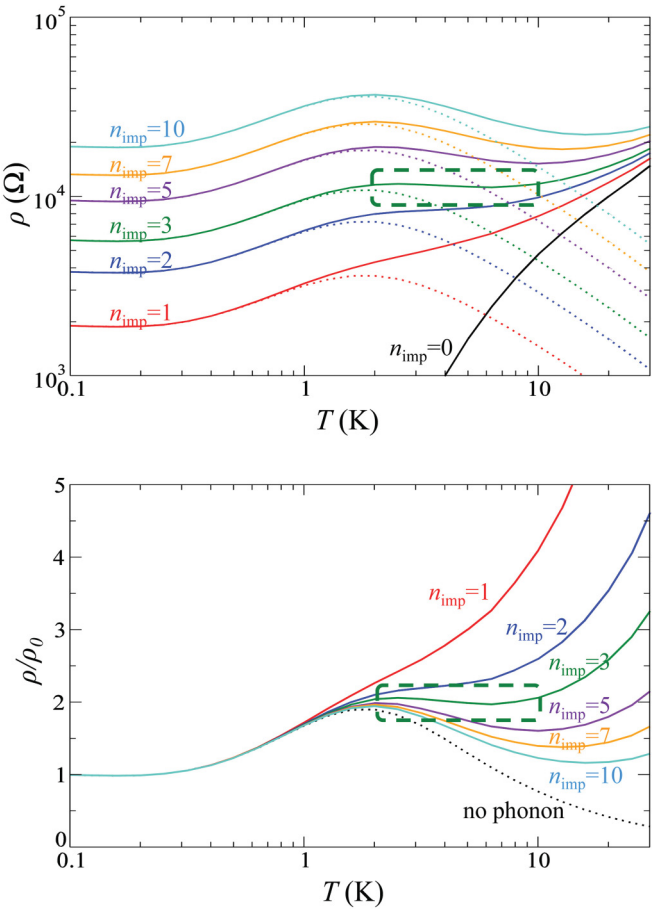

FIG. 7. (Color online) (a) Resistivity of 2DHS as a function of temperature for $n_{imp} = 0,1,2,3,5,7,10 \times 10^9$ cm^{-2} with $n = 10^{10}$ cm^{-2}, $n_{depl} = 0$, and $d_{imp} = 0$. Dotted lines indicate the calculated resistivity due to the charged impurity scattering alone. (b) Same as (a) but rescaled by $\rho_0 = \rho(T = 0.1$ K).

the temperature range 10 K $< T <$ 60 K. The slope α first increases with n, reaches its maximum at $n \sim 10^{11}$ cm^{-2}, and decreases very slowly for $n \gtrsim 10^{11}$ cm^{-2}. This nonmonotonic behavior is different from that of the n-type GaAs, in which the slope α has a minimum value rather than a maximum.[5,30]

C. Nonmonotonic resistivity in *p*-GaAs

In this subsection we study the transport in the presence of both acoustic-phonon and impurity scatterings and the nonmonotonic behavior in temperature due to the competition between these two scatterings. In Figs. 7 and 8 we show our calculated total resistivity $\rho(T)$ arising from screened charged impurity scattering $\rho_{imp}(T)$ and phonon scattering $\rho_{ph}(T)$ as a function of temperature. In Fig. 7(a) the total resistivity $\rho(T)$ is shown for different impurity densities $n_{imp} = 0,1,2,3,5,7,10 \times 10^9$ cm^{-2} with a fixed $d_{imp} = 0$. In Fig. 8(a) the total resistivity $\rho(T)$ is shown for different impurity location from the interface $d_{imp} = 0,5,10,15,20,25,30$ nm with a fixed impurity density $n_{imp} = 5 \times 10^9$ cm^{-2}. Figures 7(b) and 8(b) are the same as Figs. 7(a) and 8(a), respectively, but rescaled by $\rho_0 = \rho(T = 0.1$ K). In a real system the amount of random disorder depends on the strength and the spatial distribution of all the random impurity scattering centers. However, in these calculations we assume that the charged impurities are randomly distributed in a 2D plane located at d_{imp} from the interface. The calculation is carried out with the hole density $n = 10^{10}$ cm^{-2} which corresponds to the Fermi temperature $T_F \approx 0.7$ K. The dotted lines in Figs. 7 and 8 indicate the calculated resistivity due to the charged impurity scattering alone, $\rho_{imp}(T)$. To calculate the total resistivity $\rho(T)$ we use the total scattering rate of Eq. (24) because Matthiessen'âs rule, which is implicitly assumed $\rho(T) = \rho_{imp}(T) + \rho_{ph}(T)$, is known to be not strictly valid at finite temperatures.

As shown in Fig. 7, when the charged impurity density n_{imp} increases the impurity scattering effects become stronger, while the phonon-scattering effects are unaffected. Therefore at high impurity densities the impurity scatterings are dominant over phonon scatterings. The calculated $\rho(T)$ increases at lower temperatures ($T <$ 1 K) due to screening effects, then the quantum-classical crossover occurs at the intermediate-temperature regime around $T \sim 1.5$ K where nondegeneracy effects make resistivity decrease as $\rho \sim T^{-1}$. At higher temperatures ($T \gg 10$ K) phonon scattering takes over and $\rho(T)$ increases with T. Thus for large impurity densities the temperature dependence of the calculated resistivity shows a nontrivial nonmonotonic behavior, arising from a competition among three mechanisms discussed above, i.e., screening

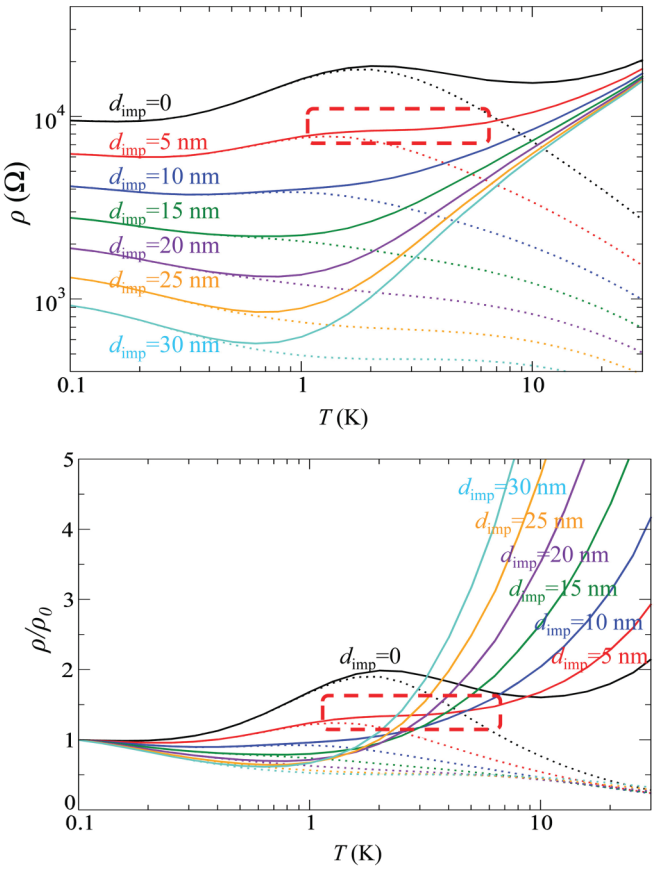

FIG. 8. (Color online) (a) Resistivity of 2DHS as a function of temperature for $d_{imp} = 0,5,10,15,20,25,30$ nm with $n = 10^{10}$ cm^{-2}, $n_{imp} = 5 \times 10^9$ cm^{-2}, and $n_{depl} = 0$. Dotted lines indicate the calculated resistivity due to the charged impurity scattering alone. (b) Same as (a) but rescaled by $\rho_0 = \rho(T = 0.1\ \text{K})$.

which is particularly important for $T < 1$ K, nondegeneracy and the associated quantum-classical crossover for $T \sim T_F$, and the phonon-scattering effect which becomes increasingly important for $T > 10$ K. At lower impurity densities the quantum-classical crossover effects are not particularly shown in Fig. 7 because phonon scattering becomes more important than the classical behavior $\rho \sim T^{-1}$, and the system makes a transition from the quantum regime to the phonon-scattering dominated regime. The linear rise in $\rho(T)$ for $T > 10$ K in Fig. 7 is the phonon-scattering effect.

The same results shown in Fig. 7 are expected by varying the impurity location because the scattering limited by the remote impurity becomes weaker as the distance of the impurity from the interface increases. In Fig. 8 we show the several different kinds of nonmonotonic behavior by varying the impurity location. When the impurities are located very close to the interface (top lines in Fig. 8) the nonmonotonic behavior of the resistivity clearly appears in the temperature range we consider (i.e., $T < 100$ K) due to competition among the three mechanisms discussed above. As the separation increases the nonmonotonicity becomes weaker because of the reduction of the charged impurity scattering and the associated weakening of screening effects. In addition, the increase of the separation gives rise to the shift of the local maximum peak to the lower temperature. For large separations (bottom lines in Fig. 8) the local maximum peak does not appear in the calculated resistivity because it shifts to very low temperatures ($T < 0.1$ K).

One interesting finding in our calculation is the temperature region where the calculated resistivity is approximately constant, as indicated by the dashed box in Figs. 7 and 8. The temperature range of the constant resistivity appears when the increasing resistivity due to phonon scatterings compensates for the decreasing resistivity due to the nondegeneracy effects. The flat region depends critically on the impurity density and the location of the impurities, and can be observed in experiments by varying the doping density and location. In Fig. 7 a flat region spanning around 2 K $< T <$ 10 K appears at an impurity density $n_{imp} = 3 \times 10^9$ cm^{-2} for $d_{imp} = 0$. In Fig. 8 the flat region for 2 K $< T <$ 10 K appears at $d_{imp} = 5$ nm with an impurity density $n_{imp} = 5 \times 10^9$ cm^{-2}. It is therefore possible in some situations for a complete accidental cancellation between the increasing temperature dependence of the phonon-induced resistivity and the decreasing temperature dependence of the quantum classical crossover effect from impurity scattering in a narrow intermediate temperature regime. We believe that this has recently been observed experimentally,[6] but a detailed comparison with experiment is not possible due to the complications of the parallel magnetic field used in the experimental measurement to induce magneto-orbital coupling.

V. CONCLUSION

To conclude, we have calculated the temperature-dependent transport properties of p-type GaAs-based 2DHSs for temperatures $T \lesssim 100$ K by taking into account both hole-phonon and hole-impurity scatterings. Our theory includes temperature-dependent screening of both charged impurity scattering and phonon scattering. We extract the deformation potential D of the hole-phonon coupling constant by fitting the experimentally available mobility data. We find that the deformation potential coupling varies (i.e., $D = 7.6$–12.7 eV) depending on the value of the depletion density n_{depl}, which is not known. When we assume $n_{depl} = 0$ we obtain $D = 12.7$ eV for the p-GaAs acoustic-phonon deformation potential, which is larger than the generally accepted value in bulk GaAs ($D = 7$ eV),[15] but comparable to the value of the n-GaAs (12–14 eV),[8,16,17] in 2D electron systems.

We also investigate the nonmonotonicity of $\rho(T)$ arising from the competition among three mechanisms: screening, nondegeneracy, and phonon scattering. Both screening and phonon-scattering mechanisms give rise to monotonically increasing $\rho(T)$ with T (at low temperature for screening, and at high temperatures for phonons), but nondegeneracy effects produce a $\rho(T)$ decreasing with increasing T for $T > T_F$. Since phonon scattering is the dominant temperature-dependent scattering mechanism in GaAs holes for $T \gtrsim$ 5–10 K, depending on the density, the stronger nonmonotonicity appears when the impurity scattering is dominant over phonon scattering below $T \sim 5$–10 K. We carefully study the nontrivial transport properties of p-GaAs at the intermediate temperature range (i.e., 2 K $< T <$ 10 K). Interestingly we find that the approximate temperature independence may appear in which $\rho(T)$ saturates in an intermediate-temperature

range, arising from the approximate cancellation between the quantum-classical crossover and phonon scattering. Since this flat region of the temperature-dependent resistivity depends critically on the impurity density and the location of the impurities, it can be observed in experiments by varying the doping density and location. We believe that a recent measurement[6] has observed this saturation effect. We note that the approximate effective model we use is the proper model in the low-density hole systems, and more importantly our qualitative finding of the appearance of the plateau structure is completely independent of the model because it arises from the competition between between the quantum-classical crossover and phonon scattering.

ACKNOWLEDGMENTS

The work was supported by the NRI-SWAN and US-ONR. We thank H. Noh for sharing unpublished data with us.

[1] J. M. Ziman, *Electrons and Phonons* (Oxford University Press, New York, 1963).
[2] E. H. Hwang and S. Das Sarma, Phys. Rev. B **77**, 115449 (2008); H. Min, E. H. Hwang, and S. Das Sarma, *ibid.* **83**, 161404 (2011); D. K. Efetov and P. Kim, Phys. Rev. Lett. **105**, 256805 (2010).
[3] Y. Hanein, U. Meirav, D. Shahar, C. C. Li, D. C. Tsui, and H. Shtrikman, Phys. Rev. Lett. **80**, 1288 (1998); M. Y. Simmons, A. R. Hamilton, M. Pepper, E. H. Linfield, P. D. Rose, D. A. Ritchie, A. K. Savchenko, and T. G. Griffiths, *ibid.* **80**, 1292 (1998); J. Yoon, C. C. Li, D. Shahar, D. C. Tsui, and M. Shayegan, *ibid.* **82**, 1744 (1999); M. J. Manfra, E. H. Hwang, S. Das Sarma, L. N. Pfeiffer, K. W. West, and A. M. Sergent, *ibid.* **99**, 236402 (2007).
[4] A. P. Mills, Jr., A. P. Ramirez, L. N. Pfeiffer, and K. W. West, Phys. Rev. Lett. **83**, 2805 (1999).
[5] T. Kawamura and S. Das Sarma, Phys. Rev. B **45**, 3612 (1992).
[6] X. Zhou, B. Schmidt, L. W. Engel, G. Gervais, L. N. Pfeiffer, K. W. West, and S. Das Sarma, Phys. Rev. B **85**, 041310 (2012).
[7] X. Zhou, B. A. Piot, M. Bonin, L. W. Engel, S. Das Sarma, G. Gervais, L. N. Pfeiffer, and K. W. West, Phys. Rev. Lett. **104**, 216801 (2010); S. Das Sarma and E. H. Hwang, *ibid.* **84**, 5596 (2000).
[8] T. Kawamura and S. Das Sarma, Phys. Rev. B **42**, 3725 (1990).
[9] S. Das Sarma and E. H. Hwang, Phys. Rev. B **61**, R7838 (2000).
[10] S. Das Sarma and E. H. Hwang, Solid State Commun. **135**, 579 (2005).
[11] E. Abrahams, S. V. Kravchenko, and M. P. Sarachik, Rev. Mod. Phys. **73**, 251 (2001).
[12] S. Das Sarma and E. H. Hwang, Phys. Rev. Lett. **83**, 164 (1999).
[13] G. Zala, B. N. Narozhny, and I. L. Aleiner, Phys. Rev. B **64**, 214204 (2001).
[14] Hwayong Noh, M. P. Lilly, D. C. Tsui, J. A. Simmons, E. H. Hwang, S. Das Sarma, L. N. Pfeiffer, and K. W. West, Phys. Rev. B **68**, 165308 (2003); H. Noh *et al.* (unpublished).
[15] C. M. Wolfe, G. E. Stillman, and W. T. Lindley, J. Appl. Phys. **41**, 3088 (1970).
[16] P. J. Price, Phys. Rev. B **32**, 2643 (1985).
[17] E. E. Mendez, P. J. Price, and M. Heiblum, Appl. Phys. Lett. **45**, 294 (1984).
[18] M. P. Lilly, J. L. Reno, J. A. Simmons, I. B. Spielman, J. P. Eisenstein, L. N. Pfeiffer, K. W. West, E. H. Hwang, and S. Das Sarma, Phys. Rev. Lett. **90**, 056806 (2003).
[19] T. Ando, A. B. Fowler, and F. Stern, Rev. Mod. Phys. **54**, 437 (1982).
[20] H. L. Stormer, Z. Schlesinger, A. Chang, D. C. Tsui, A. C. Gossard, and W. Wiegmann, Phys. Rev. Lett. **51**, 126 (1983).
[21] Y.-Ch. Chang and R. B. James, Phys. Rev. B **39**, 12672 (1989); R. Ferreira and G. Bastard, *ibid.* **43**, 9687 (1991).
[22] J. D. Watson, S. Mondal, G. Gardner, G. A. Csathy, and M. J. Manfra, Phys. Rev. B **85**, 165301 (2012); S. K. Lyo, *ibid.* **70**, 153301 (2004); E. H. Hwang and S. Das Sarma, *ibid.* **78**, 075430 (2008); C. E. Yasin, T. L. Sobey, A. P. Micolich, A. R. Hamilton, M. Y. Simmons, W. R. Clarke, L. N. Pfeiffer, K. W. West, E. H. Linfield, M. Pepper, and D. A. Ritchie, *ibid.* **72**, 241310 (2005); Y. Y. Proskuryakov, A. K. Savchenko, S. S. Safonov, M. Pepper, M. Y. Simmons, and D. A. Ritchie, Phys. Rev. Lett. **89**, 076406 (2002).
[23] F. F. Fang and W. E. Howard, Phys. Rev. Lett. **16**, 797 (1966).
[24] J. D. Zook, Phys. Rev. A **136**, 869 (1964); P. J. Price, Phys. Rev. B **32**, 2643 (1985).
[25] S. Das Sarma, S. Adam, E. H. Hwang, and E. Rossi, Rev. Mod. Phys. **83**, 407 (2011).
[26] S. Das Sarma and E. H. Hwang, Phys. Rev. B **69**, 195305 (2004); **68**, 195315 (2003).
[27] H. L. Störmer, A. C. Gossard, W. Wiegmann, R. Blondel, and K. Baldwin, Appl. Phys. Lett. **44**, 139 (1984); E. E. Mendez and W. I. Wang, *ibid.* **46**, 1159 (1985); K. Oe and K. Tsubaki, J. Appl. Phys. **59**, 3527 (1986).
[28] S. Das Sarma and F. Stern, Phys. Rev. B **32**, 8442 (1985); E. H. Hwang and S. Das Sarma, *ibid.* **77**, 195412 (2008).
[29] J. P. Harrang, R. J. Higgins, R. K. Goodall, P. R. Jay, M. Laviron, and P. Delescluse, Phys. Rev. B **32**, 8126 (1985); R. G. Mani and J. R. Anderson, *ibid.* **37**, 4299 (1988); M. Sakowicz, J. Lusakowski, K. Karpierz, M. Grynberg, and B. Majkusiak, Appl. Phys. Lett. **90**, 172104 (2007).
[30] J. J. Harris, C. T. Foxon, D. Hilton, J. Hewett, C. Roberts, and S. Auzoux, Surf. Sci. **229**, 113 (1990).